# Prospects for detecting and localizing short-duration transient gravitational waves from glitching neutron stars without electromagnetic counterparts

Dixeena Lopez,<sup>1</sup> Shubhanshu Tiwari,<sup>1</sup> Marco Drago,<sup>2,3</sup> David

Keitel.<sup>4</sup> Claudia Lazzaro,<sup>5,6</sup> and Giovanni Andrea Prodi<sup>7</sup>

<sup>1</sup>Physik-Institut, University of Zurich, Winterthurerstrasse 190, 8057 Zurich, Switzerland

<sup>2</sup>Dipartimento di Fisica, Università di Roma "La Sapienza", Piazzale Aldo Moro 2, I-00185 Roma, Italy

<sup>3</sup>INFN, Sezione di Roma, Piazzale Aldo Moro 2, I-00185 Roma, Italy <sup>4</sup>Dementement de E(inc. Universited de la Universit

Departament de Física, Universitat de les Illes Balears,

IAC3 - IEEC Crta. Valldemossa km 7.5, E-07122 Palma, Spain

<sup>5</sup> Università degli Studi di Padova

<sup>6</sup>INFN sezione di Padova

<sup>7</sup>University of Trento, Physics Department and INFN,

Trento Institute for Fundamental Physics and Applications, via Sommarive 14, 38123 Povo, Trento, Italy

Neutron stars are known to show accelerated spin-up of their rotational frequency called a glitch. Highly magnetized rotating neutron stars (pulsars) are frequently observed by radio telescopes (and in other frequencies), where the glitch is observed as irregular arrival times of pulses which are otherwise very regular. A glitch in an isolated neutron star can excite the fundamental (f)-mode oscillations which can lead to gravitational wave generation. This gravitational wave signal associated with stellar fluid oscillations has a damping time of a few seconds and occurs at the frequency range between  $1.5 - 3 \,\mathrm{kHz}$ , which is within the detectable range of the current generation of ground-based detectors. Electromagnetic observations of pulsars (and hence pulsar glitches) require the pulsar to be oriented so that the jet is pointed towards the detector, but this is not a requirement for gravitational wave emission which is more isotropic and not jet-like. Hence, gravitational wave observations have the potential to uncover nearby neutron stars where the jet is not pointed towards the earth. In this work, we study the prospects of finding glitching neutron stars using a generic all-sky search for short-duration gravitational wave transients. We set upper limits for the third observing run of the LIGO-Virgo detectors and present the prospects for upcoming observing runs of LIGO, Virgo, KAGRA, and LIGO India. We find the detectable glitch size will be around  $10^{-5}$  Hz for the fifth observing run for pulsars with spin frequency and distance comparable to the Vela pulsar. We also present the prospects of localizing the direction in the sky of these sources with gravitational waves alone, which can facilitate electromagnetic follow-up. We find that for the five detector configuration, the localization capability for a glitch size of  $10^{-5}$  Hz is around 200 square degrees at  $1\sigma$ confidence for 50% of events with distance and spin frequency as that of Vela.

#### I. INTRODUCTION

Neutron stars (NSs) are one of the most promising and versatile sources of gravitational waves (GWs) [1], including both isolated NSs and those in binary systems with other compact objects. Several searches use varied methods for different scenarios depending on the nature of the targeted GW signals. Advanced LIGO [2] and Advanced Virgo [3] have detected GW signals from compact binary coalescences (CBCs), including binary neutron star coalescences (BNSs) and neutron star-black hole coalescences (NSBHs) [4–6]. Non-radial oscillation modes, magnetic or thermal mountains for both isolated NSs and those in binaries, as well as accretion in binary systems are among the sources for continuous GWs [7]. Isolated NSs are also an interesting astrophysical source for transient GWs in the detectable range of current generation GW detectors. For example, searches have been conducted for magnetars that can be strong emitters of transient GWs and short bursts of  $\gamma$ -rays [8, 9], but no evidence of GW detection has been made to date.

In this paper, we will focus on transient GWs from glitching pulsars. Rotating isolated NSs, including pulsars, generally show a decrease in their spin frequency

over time. However, some exhibit a sudden jump in their rotation frequency known as glitches [10]. So far, 717 glitches from 239 known pulsars have been reported with glitch sizes of  $\Delta \nu_s \approx 10^{-9} - 10^{-5} \text{ Hz} [11 - 14].$ 

Glitches in isolated neutron stars can excite acoustic and inertial stellar oscillations which in turn generate GWs lasting  $\leq 0.1$  s at frequencies from 1–3 kHz. f-mode oscillations are among these potential causes of GW emission [15, 16]. Recently, also a scenario for GWs from fmodes in smaller glitch candidate events was studied in [17]. Historically, a first targeted search for short transient GWs associated with a glitch was conducted for a Vela pulsar glitch in August 2006, finding no evidence of GWs [18]. More recently, a generic all-sky search for GW transients during the third observing run [19] was also interpreted under the glitch scenario, providing a limit on minimum detectable glitch size around  $10^{-4}$  Hz for an optimally oriented source and with Vela reference parameters. In addition, searches for longer-duration quasi-monochromatic transient GWs correlated to pulsar glitches during the second and third observing runs [20–22] also put upper limits on GW strain under that scenario. But in this paper we focus on shorter signals from *f*-modes.

In general, the population of isolated NSs observed by electromagnetic (EM) observatories is a small fraction of the actual NS population in our galaxy. Hence, allsky GW searches have the potential to find previously undiscovered NSs. Follow-up searches of GW detections by EM observation, e.g. in the X-ray and radio bands, could then help in constraining NS properties. The sky localization information from the GW search is crucial to provide an opportunity for a targeted follow-up by EM telescopes.

This paper presents the all-sky search results for shortduration transient GWs from NS glitches during the third LIGO–Virgo observing run for arbitrarily oriented sources. We provide the prospects for future runs of the current generation of GW detectors regarding the glitch size one can probe. The future observing runs are expected to include KAGRA [23], LIGO India [24], and further upgrades of Advanced LIGO and Advanced Virgo. We also present the prospects for the sky localization of these sources for the upcoming observing runs.

The paper is organized as follows. Section II describes the signal model. Section III discusses the search for short transient GW signals from glitching NSs. Section IV discusses the prospects of observing and localizing these GW signals for future ground-based detector searches. Section V discusses the results.

# II. SIGNAL MODEL

#### A. Neutron star glitch models

Two main mechanisms are considered to be responsible for pulsar glitches: starquakes and superfluid–crust interactions [25–27]. In the starquake mechanism, a change in the NS's moment of inertia occurs when it tries to retain spherical symmetry. This causes an increase in its angular velocity  $\Omega_s$  by an amount  $\Delta\Omega_s$  [18]. The change in rotational kinetic energy considering the conservation of angular momentum is given as

$$\Delta E_{\text{quake}} = 2\pi^2 I_*(\nu_{\text{s}})(\Delta \nu_{\text{s}}), \qquad (1)$$

where  $I_* \approx 10^{38} \text{ kg m}^2$  is the stellar moment of inertia and  $\nu_{\rm s} = 2\pi\Omega_{\rm s}$  is the spin frequency. An order of magnitude estimate can be obtained by comparing with fiducial values of the frequency and its change at the glitch as

$$\Delta E_{\text{quake}} \approx 1.97 \times 10^{40} \text{erg} \left(\frac{\nu_{\text{s}}}{10 \,\text{Hz}}\right) \left(\frac{\Delta \nu_{\text{s}}}{10^{-7} \,\text{Hz}}\right). \quad (2)$$

For the case of superfluid–crust interactions, the energy generated during the glitch is given as

$$\Delta E_{\rm fluid} = 4\pi^2 I_{\rm c}(\nu_{\rm s})(\Delta\nu_{\rm s})(\nu_{\rm lag}/\nu_{\rm s})\,,\tag{3}$$

where we neglect the term  $\nu_{\text{lag}}/\nu_{\text{s}} \approx 5 \times 10^{-4}$ , the rotational difference between crust and superfluid interior, and for the moment of inertia of the crust we assume  $I_c \approx I_*$  [28]. The angular momentum transfer drives the crust to spin up and the superfluid part to spin down, driving the co-rotation between the superfluid core and crust [18]. Assuming fiducial values of the parameters, the change in rotational energy can be expressed as

$$\Delta E_{\rm fluid} \approx 3.95 \times 10^{40} \rm erg\left(\frac{\nu_{\rm s}}{10\,\rm Hz}\right) \left(\frac{\Delta \nu_{\rm s}}{10^{-7}\,\rm Hz}\right) \,. \tag{4}$$

A possible consequence of NS glitches is the excitation of one or more oscillations in the NS. This leads to the excitation of different families of pulsation modes like pressure *p*-modes (the fundamental of which is known as the f-mode) and the gravity g-modes corresponding to the energy of the glitch [16, 29-31]. In this work, we are interested in the f-modes, which are the dominant mode in producing transient GWs from NS glitches [32–34]. The oscillations caused by the glitch will be at least partially damped by GW emission on a time scale of milliseconds to seconds, leading to a characteristic GW signal in the form of a decaying sinusoid [35]. For a perfectly spherical NS (non-rotating, non-magnetic), the damping time  $\tau_m$ and mode frequency  $\omega_m$  are degenerate for each mode m. Moreover, we consider only the dominant quadrupolar emission (l = 2) here as higher-order modes (l > 2) will be sub-dominant [36, 37] and also will occur at a higher frequency where the detectors lose sensitivity. The total GW energy emitted is then given as

$$\Delta E \equiv \int_0^\infty \frac{dE}{dt} dt = \frac{2\pi}{75} \sum_m \omega_m^6 \left( M R^2 \alpha_m \right)^2 \tau_m \,, \quad (5)$$

where M and R are the stellar mass and radius respectively, and the mode amplitudes  $\alpha_m$  are defined as

$$\alpha_m \equiv \frac{1}{MR^2} \int \rho_m(r) r^4 dr \,. \tag{6}$$

Neglecting the effect of rotation and magnetic fields, GWs associated with the excitation of pulsation modes (f-modes) are short-lived signals, which can be expressed in the time domain as [38]

$$h(t) = h_0 e^{-t_{\rm gw}/\tau} \sin[\omega_{\rm gw}(t_{\rm gw})].$$
(7)

Here,  $h_0$  is the initial amplitude of the signal.  $\nu_{\rm gw} = \omega_{\rm gw}/2\pi$  and  $\tau_{\rm gw}$  are the frequency and characteristic damping time of the signal, respectively.

The initial amplitude is related to GW energy emitted by a source at a distance d [39]:

$$h_0 = \frac{1}{\pi d\nu_{\rm gw}} \left(\frac{5G}{c^3} \frac{E_{\rm gw}}{\tau_{\rm gw}}\right)^{1/2} \,. \tag{8}$$

Substituting for GW energy and using  $I_* \sim 10^{38}$  kg m<sup>2</sup>, the peak GW amplitude of the f-mode ringdown signal

is

$$h_{0} = 7.21 \times 10^{-24} \left(\frac{1 \,\mathrm{kpc}}{d}\right) \left(\frac{\nu_{\mathrm{s}}}{10 \,\mathrm{Hz}}\right)^{1/2} \\ \left(\frac{\Delta \nu_{\mathrm{s}}}{10^{-7} \,\mathrm{Hz}}\right)^{1/2} \left(\frac{1 \,\mathrm{kHz}}{\nu_{\mathrm{gw}}}\right) \left(\frac{0.1 \,\mathrm{s}}{\tau_{\mathrm{gw}}}\right)^{1/2} .$$
(9)

#### B. Frequency and damping time of the signal

The frequency and characteristic damping time of a GW signal emitted by an f-mode oscillation during a glitch are related to the mean density of the NS [15, 38, 40]. We can find these relations by solving the non-radial perturbations equation of a non-rotating star in general relativity (GR) or using the Cowling approximation [41–45]. In this work, we consider the Cowling approximation [29, 46] where the perturbations of the metric are neglected and only fluid perturbations are taken into account [40].

In full GR, the perturbed metric has the form  $g_{\mu\nu} + \delta g_{\mu\nu}$  with the perturbation to the Einstein field equations taking the form

$$\delta G_{\mu\nu} = \delta (R_{\mu\nu} - \frac{1}{2} R g_{\mu\nu}) = 8\pi \delta T_{\mu\nu} ,$$
 (10)

where  $T_{\mu\nu} = (\rho + p)u_{\mu}u_{\nu} + pg_{\mu\nu}$  is the energy-momentum tensor with energy density  $\rho$  and pressure p. Assuming NSs to be made of a relativistic perfect fluid leads to the conservation law of energy-momentum  $\Delta_{\nu}T^{\mu\nu} = 0$ [47, 48]. In the Cowling approximation, taking into account that the metric is kept fixed and by varying the equation for the conservation of the energy-momentum tensor  $\Delta_{\nu}(\delta T^{\mu\nu}) = 0$  with  $\delta g_{\mu\nu} = 0$ . The solution of a linear perturbation can be decomposed into a sum of independent quasinormal modes [42]. Assuming a harmonic dependence on time with an appropriate boundary condition at the center and at the stellar surface, the density and pressure perturbations can be expressed in terms of the complex eigenfrequency of the quasinormal mode [49-51]. The solution of the perturbed equation for the complex eigenfrequency defines the quasinormal modes of the star [52-54]. The frequency and damping time of a mode due to GW emission are the real part and inverse of the imaginary part of the eigenfrequency.

Quasinormal modes are classified according to the restoring force, which brings the perturbed element of the fluid back to the equilibrium position. We consider the non-rotating limit where only GWs from f-mode oscillations are well inside the sensitive bandwidth of ground-based GW detectors [15]. Empirical relations for frequencies and damping times, fit to the mean mass density and compactness for various equations of state (EoS), are given as [40]

$$\nu_{\rm gw}[\rm kHz] = 1.562 + 1.151 \left(\frac{\bar{M}}{\bar{R}^3}\right)^{1/2}$$
 (11)

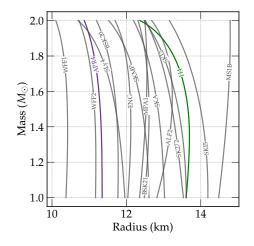


FIG. 1. The mass-radius curves for a sample of EoS, over a mass range of  $1 - 2 M_{\odot}$ . We choose the APR4 (purple) and H4 (green) EoS for this study, representing more and less compact NSs respectively.

and

$$\frac{1}{\tau_{\rm gw}[\rm s]} = \frac{\bar{M}^3}{\bar{R}^4} \left[ 78.55 - 46.71 \left(\frac{\bar{M}}{\bar{R}}\right) \right] \,, \qquad (12)$$

where

$$\bar{M} = \frac{M}{1.4M_{\odot}}$$
 and  $\bar{R} = \frac{R}{10\,\mathrm{km}}$ . (13)

Each nuclear-matter EoS generates a unique relation between the mass and radius of NSs [55]. To use the empirical relations given above for the frequency and damping time, we need that mass-radius relation. But the EoS of NSs is currently not precisely known. However, there are constraints on the EoS from radio and GW observations [56]. The mass-radius relation for non-rotating NS models with various EoS [57] for masses between  $1-2M_{\odot}$ are shown in Fig. 1. In this work, we choose two different EoS namely APR4 [58] and H4 [59], which are considered as representatives for the classes of soft (more compact) and hard (less compact) models respectively.

For both cases of EoS (APR4 and H4) we compute the relation given in equations 11 and 12 to obtain the dependency of GW signal properties (frequency and damping time) as a function of NS mass as shown in Fig. 2. For the typical masses of NSs between  $1 - 2M_{\odot}$ , we obtain corresponding f-mode frequencies between  $1-3 \,\mathrm{kHz}$  [60]. As the mass of the NS increases the f-mode frequency increases. Also, we can infer that for the softer EoS the frequencies are systematically higher than that for the harder EoS. One can speculate that a confident detection of GWs from an NS glitch with a sufficiently accurate frequency estimation will contain information about the EoS, which is degenerate with NS mass but not in the entirety of the parameter space. In Fig. 2, we also show the distribution of the damping time  $\tau_{\rm gw}$ . The damping times decrease as the mass of the NS increases and



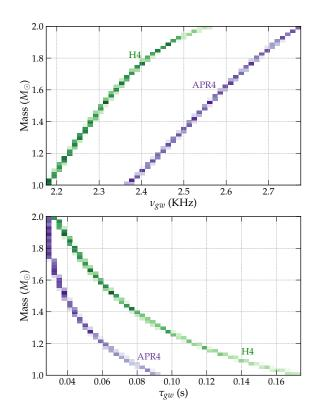


FIG. 2. GW frequency (top panel) and damping time (bottom panel) as a function of NS mass according to equations 11 and 12. Here, we consider the non-rotating limit and compare the relations for two EoSs, APR4 (purple) and H4 (green).

it should be noted that for the softer EoS the damping time drops off faster than for the harder EoS.

Furthermore, we also compare our signal model with numerical relativity simulations solving the Einstein equations for dynamical spacetimes in full GR. The fundamental mode frequency  $\nu$  in full GR with dynamical spacetime for a non-rotating star is given as

$$\nu[\text{kHz}] = k_l + \mu_l \left(\frac{\bar{M}}{\bar{R}^3}\right)^{1/2} \tag{14}$$

where  $(k_2, \mu_2) = (0.912, 29.05)$  [61, 62] for the APR4 EoS. Figure 3 shows the difference in the frequency estimate with the Cowling approximation (which we will use in our study) and full GR, depending on the mass density. We see that the difference is merely a systematic frequency shift in this particular parameterization. The Cowling approximation overestimates the f-mode frequency compared to the full GR result by around ~ 30% [15, 32]. This deviation varies for different EoS and is in general not negligible. However, since the frequency is overestimated with the Cowling approximation, using it in the following analysis can be considered a conservative choice as GW detector sensitivities in the kHz regime fall off as the frequency increases. Also, full GR simulations are only available for a limited number of EoS [1] and hence we follow most current studies in using the more widely

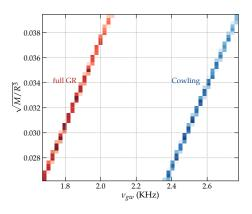


FIG. 3. Distribution of GW frequency as a function of NS density for APR4 EoS. The red curve shows the full GR approximation and the blue shows in Cowling approximation. For the given mass range and EoS, the Cowling approximation overestimates the *f*-mode frequency by 30% than full GR.

applicable Cowling approximation.

### **III. ANALYSIS OVERVIEW**

We consider an all-sky search for generic shortduration GW transients using the coherent WaveBurst (cWB) pipeline. cWB is a morphology-independent algorithm for the detection and reconstruction of GW transients. It is based on maximum likelihood-ratio statistics applied to excess power above the detector noise in the multi-resolution time-frequency (T-F) representation of GW strain data [63–65]. We use the same version of cWB as was used for the LIGO-Virgo-KAGRA collaboration's third observing run (O3) high-frequency search for generic transients [19], with the exact same settings.

As discussed in Section II and also in [15, 40], GWs from f-mode oscillations in glitching pulsars will occur in the high-frequency range (2 - 3 kHz) of ground-based detectors. Therefore, we restrict our analysis to the frequency range of 1-4 kHz. We have analyzed the publicly available O3 data, which extended from April 1, 2019 to March 1, 2020 [19, 66]. For these O3 results, we consider only the Hanford--Livingston (HL) network, since Virgo has a significant sensitivity imbalance for frequencies higher than 1 kHz (almost a factor 5). For the near future prospects of detecting GWs from NS glitches in the fourth (O4) and fifth (O5) observing runs, we have generated Gaussian noise based on the expected spectral sensitivities for the three-detector network with both LI-GOs and Virgo [67]. Fig. 4 shows the sensitivities of the detectors, in terms of measured noise amplitude spectral densities from O3 and the expected curves for O4 and O5 [68]. For O3, we have used the data from the two LIGO detectors and produced over 500 years of time-shifted background with approximately 200 days of available coincident observing time. For O4 and O5, we have simulated 16.85 days of data for the LIGO and Virgo detec-

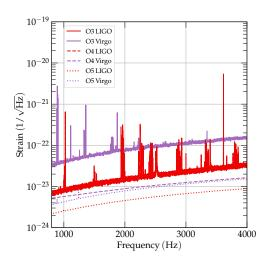


FIG. 4. Noise amplitude spectral densities of the LIGO and Virgo detectors for O3 (measured) as well as predictions for O4 and O5 in the high-frequency range.

tors by assuming Gaussian noise which follows the PSD for the corresponding detector and observing run. From this data, we have produced 23 years of background by a time-shifting of LIGO Hanford and Virgo by keeping LIGO Livingston as a reference. For O3, the most significant trigger had an inverse False Alarm rate of about 1 event in 0.3 years which is well within the expected background rate (assuming the detectors' glitches follow a Poisson distribution, the significance is 0.5 sigma).The central frequency of this trigger was 2.1 kHz [19].

To compute the detection sensitivity of this highfrequency all-sky search setup with a given detector configuration, we perform an injection study of adding simulated damped sinusoid waveforms to the data. In this work, we have used a different (more realistic) injection set in terms of the extrinsic parameters of the signals as compared to the results presented in [19]. In [19], the distribution of the simulated sources in the sky was uniform. By contrast, here we have used a distribution in sky directions that is uniform over the galactic disk based on the Miyamoto-Nagai Galactic Disk Model [69, 70]. Also, in [19] the inclination angle of all sources was chosen as face-on (optimally oriented), whereas here we sample uniformly over the full range of inclination angles.

As discussed in Section II, the parameters of the damped sinusoids (frequency and damping times) can be related to the source parameters (mass and EoS of the NS). The amplitude of the incoming signal is a function of distance to the source, spin frequency of the NS and glitch size. We fix the distance of the source to that of the Vela pulsar at 287 pc [71]. (For clarity, we underline that we do not fix the sky direction to that of Vela, just the distance.) We also fix the spin frequency of the NS to approximately that of Vela ( $\nu_{\rm s} = 11.2 \, {\rm Hz}$ ) [72].

The sensitivity is then determined using the value of the quantity  $h_{\rm rss} = \sqrt{\int_{-\infty}^{\infty} (h_+^2(t) + h_{\times}^2(t)) dt}$  needed to

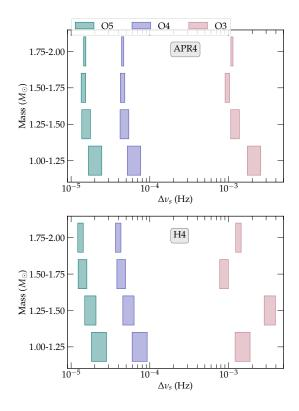


FIG. 5. Sensitivity of the high-frequency all-sky transient search during the O3 run in terms of detectable NS glitch sizes. The corresponding expected sensitivities for O4 and O5 using their predicted noise curves are also shown. Signals are simulated using the spin frequency and distance of the Vela pulsar, other source parameters are drawn from distributions as described in the text with NS models following two different EoS (APR4 and H4). The sensitivities are shown separated into four mass bins between 1-2  $M_{\odot}$ . The variation in detectable glitch size within each mass bin is indicated by the horizontal width of the box for each bin. The glitch size is computed from the minimum  $h_{\rm rss}$  needed for 50% detection efficiency at iFAR $\geq$  10 years. We consider the HL network for O3 results and the HLV network for the O4 and O5 runs.

achieve 50% detection efficiency for each mass bin and EoS, at an inverse False-Alarm Rate (iFAR) larger than 10 years. As the other parameters (distance and spin frequency) are fixed, we interpret the result in terms of glitch size  $\Delta \nu_s$  determined using equation 9. Keeping the Vela pulsar as a reference for distance and spin frequency, Fig. 5 reports the limit on detectable glitch size as a function of mass and EoS for the O3 run, as well as projected detectable glitch sizes for the future O4 and O5 sensitivities.

In [19] the detectable glitch size for optimally oriented sources (uniformly distributed in all sky directions) was greater than  $10^{-4}$  Hz. Under our more realistic source distribution, for O3 we find that we would have needed a glitch size larger than  $\approx 10^{-3}$  Hz to confidently detect 50% of events. This difference arises mainly from losing the condition for optimal orientation of the source.

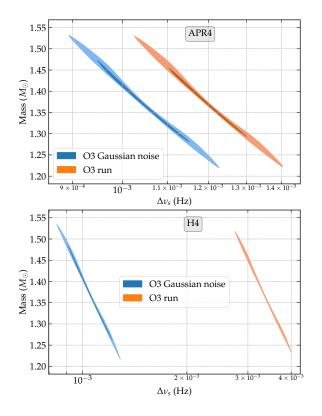


FIG. 6. Difference in detectable glitch sizes obtained from the real O3 data compared with simulated Gaussian noise at O3 detector sensitivity. The injected waveforms are for APR4 and H4 EoS with a mass range between  $1.25 - 1.50 M_{\odot}$ . It can be seen that the non-stationary lines at 2.2 - 2.3 kHz hinder the detectability of H4 EoS signals in this mass range, whereas for APR4 signals which do not fall near the non-stationary lines, detectability is similar in real data and Gaussian noise.

For O4 we see around an order of magnitude improvement for the detectable glitch size across the mass bins for both cases of EoS as compared to O3. For O5 this is around two orders of magnitude improvement in detectable glitch size. These improvements are attributed both to improvements in each detector but also to the inclusion of Virgo, which allows injections to be recovered from a wider portion of the sky.

The assumption of Gaussian noise (which we make for the future observing runs) is not too far from reality for the high-frequency range of the detectors. However, nonstationary lines [73, 74] are present in real data. These lines lead to an anomalously bad sensitivity visible in the results (Fig. 5) for the H4 EoS mass bin  $1.25 - 1.5 M_{\odot}$ . Following up on this, we found that this reduced sensitivity correlates with a population of lines occurring between 2.2 - 2.3 kHz, which reduces the sensitivity of the detectors for signals falling in this frequency range, leading to higher glitch sizes needed for detections in this mass bin.

We conducted an additional study to quantify this hypothesis that indeed the noise happening between 2.2–2.3 kHz during the O3 run causes this reduction in sensi-

tivity. For this, we generated simulated data with Gaussian noise with O3 noise spectral density [68] and computed the detectable glitch size at iFAR higher than 10 years. We found a factor of 3.35 improvement with Gaussian noise as compared to real O3 noise as, shown in Fig. 6. If we take this into account, this outlier mass bin in H4 EoS with worse sensitivity can be explained. This also outlines the fact that the main challenge for the practical implementation of this analysis in future observing runs will be the mitigation of wandering lines in the high-frequency part of the parameter space.

# IV. PROSPECTS FOR LOCALIZING GLITCHING NS FROM GW DETECTION

Since we are looking to unveil a population of nearby NSs which may not yet have been observed in the EM spectrum, sky localization of the sources of GW detections will play a key role in enabling the follow-up of this event by various ground and space based telescopes. Even if the GW signal is associated in time with an EM transient, we would still need sky direction information to unambiguously associate the events. In this section, we provide a comprehensive study on the sky localization capabilities of different networks of GW detectors.

Sky localization with a network of GW detectors relies upon the time delay measurement between various detectors. Given a pair of detectors, the time of arrival and the amplitude will localize the signal to a ring in the sky [75]. If we have three detectors and hence two pairs, we can localize a source to a much smaller region around the intersection of the two circles in the sky corresponding to each pair of detectors. Longer baselines between detectors and a higher number of detectors lead to better localization [76].

In the case of cWB the likelihood is computed and is maximized over sky directions, which is very sensitive to the time delays, antenna pattern response and polarization of incoming GWs. The reconstructed sky direction statistic is a function of the likelihood. Further discussion about the properties of the sky statistics of cWB can be found in Section 3 of [63]. The dominant source of error in the sky localization comes from the estimate of arrival times, which gets challenging for generic transient searches at high frequencies.

Here we study the prospects for localizing GW transients from a NS glitch considering the APR4 EoS for masses between  $1.25 - 1.5M_{\odot}$ , using simulated Gaussian noise for the O5 run. We inject the NS glitch waveforms in the simulated data corresponding to the spin frequency and distance of the Vela pulsar with five glitch size values logarithmically spaced between  $10^{-6}$  Hz and  $10^{-3}$  Hz. For each considered glitch size, the sources are uniformly distributed in spin direction and source orientation. We quote the results in terms of the  $1\sigma$  error in sky localization that is achieved for 50% of events. We consider the following present and future detectors: LIGO-Hanford

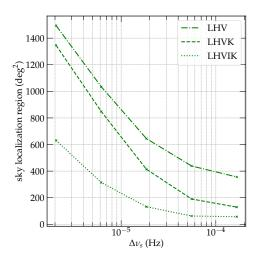


FIG. 7. Sky localization region size as a function of NS glitch size assuming O5 sensitivity for the LHVIK, LHVK, and LHV networks. Specifically, this is the localization region size at  $1\sigma$  confidence achieved by 50% of the events at a given glitch size. Here we used the APR4 EoS and NS masses between  $1.25 - 1.5M_{\odot}$  to generate simulated signals.

(H), LIGO-Livingston (L), Virgo (V), KAGRA (K), and LIGO-India (I), combining them in three different networks: LHV, LHVK, LHVIK.

We show the results in figure 7. As expected, a drastic improvement can be seen as the number of detectors in the network increases and also an improvement as the glitch size grows (since the signal-to-noise ratio grows with it). Still, for a realistic scenario of  $10^{-5}$  Hz glitch size with the five detector network, we get the sky localization region of around 200 square degrees at  $1\sigma$  for 50% of events, which might be too large for many EM telescopes to efficiently follow up the full sky area. But compared with CBC localization areas in O1–O3 [4–6], this level of localization can still provide an opportunity to potentially find an EM counterpart to a transient burst GW detection from a glitching pulsar.

## V. DISCUSSIONS

In this work, we have updated the all-sky upper limits from the LIGO–Virgo O3 run for short-duration GW signals from f-modes triggered by glitches in NSs without electromagnetic counterparts by using more realistic distributions in the extrinsic parameters (i.e. sky direction and orientation of the source) of the simulated signals used for sensitivity estimation. We have also investigated how line artifacts in the O3 data affect sensitivity in certain frequency bands and hence source mass ranges, which sheds light on the practical challenges which we face for such high-frequency shortduration searches. Further, we give the prospects for the detection and localization of such short-duration GWs from NS glitches for the upcoming fourth (O4) and fifth

(O5) observing runs of the current generation of groundbased detectors. By fixing the reference pulsar as Vela (in terms of distance and spin frequency) we found that the detectable glitch size will be around  $10^{-4}$  Hz for O4 and  $10^{-5}$  Hz for O5. Glitch sizes of the  $10^{-5}$  Hz have been observed by radio telescopes before [11, 72, 77]. Further, it has been shown that observed pulsar glitches form two different populations when it comes to glitch size [10, 78, 79]. These distributions are conventionally called normal or Crab-like for the smaller glitches and Vela-like for the larger (mean at around  $10^{-4.4}$  Hz) glitches. Thus, for O4 and O5 there can be a more realistic chance to observe a nearby glitching pulsar if the glitch comes from the population of Vela-like glitches. We have also studied the localization capability of this type of GW searches, finding that with a five detector network during O5 for the detectable glitch sizes of  $10^{-5}$  Hz the EM follow up can be challenging, as the sky error region for 50% events at  $1\sigma$  is about 200 square degrees. However, this localization can still be useful for future wide-scope telescopes like CHIME, SKA, etc [80, 81]. It could also be sufficient to associate the GW event with the galactic disk.

The proposed third-generation GW observatories like Einstein Telescope [82], Cosmic Explorer [83], and NEMO [84] will provide much high sensitivities at kHz ranges, ideal for observing GW signals from glitching pulsars. We leave it for future studies to quantify the sensitivity of third generation detectors where the analysis methods and search configurations will need to be very different.

## ACKNOWLEDGMENTS

We thank Leigh Smith for her comments on an early version of this draft. The document has been given LIGO DCC number P2200190. DL acknowledges support from Swiss National Science Foundation (SNSF) grant number 200020-182047. ST is supported by Swiss National Science Foundation (SNSF) Ambizione Grant Number : PZ00P2-202204. MD acknowledges the support from the Amaldi Research Center funded by the MIUR program 'Dipartimento di Eccellenza' (CUP:B81I18001170001) and the Sapienza School for Advanced Studies (SSAS).

DK is supported by the Spanish Ministerio de Ciencia, Innovación y Universidades (ref. BEAGAL 18/00148) and cofinanced by the Universitat de les Illes Balears, and acknowledges support by European Union FEDER funds, the Spanish Ministerio de Ciencia e Innovación and Spanish Agencia Estatal de Investigación grants PID2019-106416GB-I00/AEI/MCIN/10.13039/501100011033, DED2018 102661 T. DED2018 102572 E the Comunitat

RED2018-102661-T, RED2018-102573-E, the Comunitat Autònoma de les Illes Balears through the Conselleria de Fons Europeus, Universitat i Cultura and the Direcció General de Política Universitaria i Recerca with funds from the Tourist Stay Tax Law ITS 2017-006 (PRD2018/24, PRD2020/11), the Generalitat Valenciana (PROMETEO/2019/071), and EU COST Actions

## CA18108, CA17137 and CA16214.

This research has made use of data obtained from the Gravitational Wave Open Science Center (https://www.gw-openscience.org), a service of LIGO Laboratory, the LIGO Scientific Collaboration and the Virgo Collaboration. The authors are grateful for the

- K. Glampedakis and L. Gualtieri, "Gravitational waves from single neutron stars: An advanced detector era survey," in *The Physics and Astrophysics of Neutron Stars*, edited by L. Rezzolla *et al.* (Springer International Publishing, Cham, 2018) pp. 673–736.
- [2] J. Aasi *et al.*, Classical and Quantum Gravity **32**, 074001 (2015).
- [3] F. Acernese *et al.*, Classical and Quantum Gravity **32**, 024001 (2014).
- [4] B. P. Abbott *et al.* (LIGO Scientific Collaboration and Virgo Collaboration), Phys. Rev. X 9, 031040 (2019).
- [5] R. Abbott *et al.* (LIGO Scientific Collaboration and Virgo Collaboration), Phys. Rev. X 11, 021053 (2021).
- [6] R. Abbott *et al.* (LIGO Scientific Collaboration, Virgo Collaboration and KAGRA Collaboration), (2021), arXiv:2111.03606.
- [7] K. Riles, arXiv:2206.06447.
- [8] B. P. Abbott *et al.* (LIGO Scientific Collaboration and Virgo Collaboration), Astrophys. J. 874, 163 (2019).
- [9] R. Abbott *et al.* (LIGO Scientific Collaboration, Virgo Collaboration, and KAGRA Collaboration), Astrophys. J. 928, 186 (2022).
- [10] J. R. Fuentes, C. M. Espinoza, A. Reisenegger, B. W. Stappers, B. Shaw, and A. G. Lyne, Astron. Astrophys. 608, A131 (2017).
- [11] C. M. Espinoza, A. G. Lyne, B. W. Stappers, and M. Kramer, Mon. Not. R. Astron. Soc. 414, 1679 (2011).
- [12] A. Basu *et al.*, Mon. Not. R. Astron. Soc. **510**, 4049 (2021).
- [13] B. Shaw, A. Lyne, M. Mickaliger, et al., "Jodrell Bank Pulsar Glitch Catalogue," http://www.jb.man.ac.uk/ pulsar/glitches.html (2022).
- [14] G. B. Hobbs, R. N. Manchester, and L. Toomey, "The Australia Telescope National Facility Pulsar Catalogue: Glitch Parameters," https://www.atnf.csiro. au/people/pulsar/psrcat/glitchTbl.html (2022).
- [15] N. Andersson and K. D. Kokkotas, Mon. Not. R. Astron. Soc. 299, 1059 (1998).
- [16] W. C. G. Ho, D. I. Jones, N. Andersson, and C. M. Espinoza, Phys. Rev. D 101, 103009 (2020).
- [17] G. Yim and D. I. Jones, arXiv:2204.12869.
- [18] J. Abadie *et al.* (LIGO Scientific Collaboration), Phys. Rev. D 83, 042001 (2011).
- [19] R. Abbott *et al.* (LIGO Scientific Collaboration, Virgo Collaboration and KAGRA Collaboration), Phys. Rev. D 104, 122004 (2021).
- [20] D. Keitel et al., Phys. Rev. D 100, 064058 (2019).
- [21] R. Abbott *et al.* (LIGO Scientific Collaboration, Virgo Collaboration and KAGRA Collaboration), (2021), arXiv:2112.10990.
- [22] L. M. Modafferi, J. Moragues, and D. Keitel (for the LIGO Scientific, Virgo and KAGRA collaborations), J. Phys. Conf. Ser. 2156, 012079 (2021).

computational resources provided by the LIGO Lab (CIT) and supported by National Science Foundation Grants PHY-0757058 and PHY-0823459. This material is based upon work supported by NSF's LIGO Laboratory which is a major facility fully funded by the National Science Foundation.

- [23] T. Akutsu *et al.* (KAGRA Collaboration), Progress of Theoretical and Experimental Physics **2021** (2020).
- [24] B. R. Iyer *et al.*, *LIGO-India*, Tech. Rep. LIGO-M1100296 (IndIGO, 2011).
- [25] B. Haskell and A. Melatos, Int. J. Mod. Phys. D 24, 1530008 (2015).
- [26] E. Stopnitzky and S. Profumo, Astrophys. J. 787, 114 (2014).
- [27] T. Sidery, A. Passamonti, and N. Andersson, Mon. Not. R. Astron. Soc. 405, 1061 (2010).
- [28] R. Prix, S. Giampanis, and C. Messenger, Phys. Rev. D 84, 023007 (2011).
- [29] T. G. Cowling, Mon. Not. R. Astron. Soc. 101, 367 (1941).
- [30] K. D. Kokkotas and B. G. Schmidt, Living Rev. Relativity. 2, 2 (1999).
- [31] N. Andersson and G. Comer, Phys. Rev. Lett. 87, 241101 (2001).
- [32] V. Ferrari, G. Miniutti, and J. A. Pons, Mon. Not. R. Astron. Soc. 342, 629 (2003).
- [33] D. Lai, Mon. Not. R. Astron. Soc. **307**, 1001 (1999).
- [34] C. J. Krüger, W. C. G. Ho, and N. Andersson, Phys. Rev. D 92, 063009 (2015).
- [35] C. Peralta, A. Melatos, M. Giacobello, and A. Ooi, Astrophys. J. 651, 1079 (2006).
- [36] I. Jones, Calculating gravitational waveforms: examples, Tech. Rep. LIGO-T1200476 (LIGO Laboratory, 2021).
- [37] K. S. Thorne, Rev. Mod. Phys. **52**, 299 (1980).
- [38] K. D. Kokkotas and N. Andersson, in 14th SIGRAV Congress on General Relativity and Gravitation (SIGRAV 2000) (2002) pp. 121–139.
- [39] J. A. de Freitas Pacheco, Astron. Astrophys. 336, 397, arXiv:astro-ph/9805321.
- [40] E. Doneva, Daniela D. Gaertig, K. Kokkotas, and C. Krüger, Phys. Rev. D 88, 044052 (2013).
- [41] B. Zink, O. Korobkin, E. Schnetter, and N. Stergioulas, Phys. Rev. D 81, 084055 (2010).
- [42] G. Lioutas and N. Stergioulas, Gen. Rel. Grav. 50, 12 (2018).
- [43] P. N. McDermott, H. M. van Horn, and J. F. Scholl, Astrophys. J. 268, 837 (1983).
- [44] L. Lindblom and R. J. Splinter, Astrophys. J. 348, 198 (1990).
- [45] S. Yoshida and Y. Kojima, Mon. Not. R. Astron. Soc. 289, 117 (1997).
- [46] P. N. McDermott, H. M. van Horn, and J. F. Scholl, Astrophys. J. 268, 837 (1983).
- [47] S. G. Rosofsky, R. Gold, C. Chirenti, E. A. Huerta, and M. C. Miller, Phys. Rev. D 99, 084024 (2019).
- [48] S. L. Detweiler, Astrophys. J. 197, 203 (1975).
- [49] H. Sotani, Phys. Rev. D 79, 064033 (2009).
- [50] D. D. Doneva and S. S. Yazadjiev, Phys. Rev. D 85, 124023 (2012).
- [51] S. S. Yazadjiev and D. D. Doneva, JCAP 03, 037 (2012).

- [52] S. Chandrasekhar and V. Ferrari, Proc. Roy. Soc. Lond. A 432, 247 (1991).
- [53] S. Chandrasekhar, V. Ferrari, and R. Winston, Proc. Roy. Soc. Lond. A 434, 635 (1991).
- [54] O. Benhar, V. Ferrari, and L. Gualtieri, Phys. Rev. D 70, 124015 (2004).
- [55] A. W. Steiner, J. M. Lattimer, and E. F. Brown, Astrophys. J. 765, L5 (2013).
- [56] J. M. Lattimer, Annu. Rev. Nucl. Part. Sci. 71, 433 (2021).
- [57] F. Özel, D. Psaltis, T. Güver, G. Baym, C. Heinke, and S. Guillot, Astrophys. J. 820, 28 (2016).
- [58] A. Akmal, V. R. Pandharipande, and D. G. Ravenhall, Phys. Rev. C 58, 1804 (1998).
- [59] B. D. Lackey, M. Nayyar, and B. J. Owen, Phys. Rev. D 73, 024021 (2006).
- [60] S. Jaiswal and D. Chatterjee, MDPI Physics 3, 302 (2021).
- [61] C. Chirenti, G. H. de Souza, and W. Kastaun, Phys. Rev. D 91, 044034 (2015).
- [62] S. Shashank, F. H. Nouri, and A. Gupta, arXiv:2108.04643.
- [63] S. Klimenko, G. Vedovato, M. Drago, F. Salemi, V. Tiwari, G. A. Prodi, C. Lazzaro, K. Ackley, S. Tiwari, C. F. Da Silva, and G. Mitselmakher, Phys. Rev. D 93, 042004 (2016).
- [64] M. Drago et al., SoftwareX 14, 100678 (2021).
- [65] https://gwburst.gitlab.io.
- [66] R. Abbott et al., SoftwareX 13, 100658 (2021).
- [67] B. P. Abbott *et al.* (LIGO Scientific Collaboration, Virgo Collaboration and KAGRA Collaboration), Living Rev. Relativity. 23, 3 (2020).
- [68] B. P. Abbott et al. (LIGO Scientific Collaboration, Virgo

Collaboration and KAGRA Collaboration), Noise curves used for Simulations in the update of the Observing Scenarios Paper, Tech. Rep. LIGO-T2000012 (LIGO Laboratory, 2022).

- [69] M. Miyamoto and R. Nagai, Publ. Astron. Soc. Jap. 27, 533 (1975).
- [70] D. A. Barros, J. R. D. Lépine, and W. S. Dias, Astron. Astrophys. 593, A108 (2016).
- [71] R. Dodson, D. Legge, J. E. Reynolds, and P. M. McCulloch, Astrophys. J. 596, 1137 (2003).
- [72] R. N. Manchester, G. B. Hobbs, A. Teoh, and M. Hobbs, Astron. J. **129**, 1993 (2005).
- [73] P. B. Covas *et al.* (LSC Instrument Authors), Phys. Rev. D 97, 082002 (2018).
- [74] D. Davis *et al.*, Classical and Quantum Gravity 38, 135014 (2021).
- [75] R. Essick, S. Vitale, E. Katsavounidis, G. Vedovato, and S. Klimenko, Astrophys. J. 800, 81 (2015).
- [76] C. Pankow, E. A. Chase, S. Coughlin, M. Zevin, and V. Kalogera, Astrophys. J. Lett. 854, L25 (2018).
- [77] M. Yu et al., Mon. Not. R. Astron. Soc. 429, 688 (2013).
- [78] G. Ashton, R. Prix, and D. I. Jones, Phys. Rev. D 96, 063004 (2017).
- [79] S. Arumugam and S. Desai, arXiv:2206.02751.
- [80] J. R. Shaw, K. Sigurdson, U.-L. Pen, A. Stebbins, and M. Sitwell, Astrophys. J. 781, 57 (2014).
- [81] A. Weltman *et al.*, Publ. Astron. Soc. Austral. **37**, e002 (2020).
- [82] ET Science Team, "Einstein gravitational wave Telescope conceptual design study," (2011), eT-0106C-10.
- [83] M. Evans et al., arXiv:2109.09882.
- [84] K. Ackley et al., Publ. Astron. Soc. Austral. 37, e047 (2020).